

# Fermi Constrains Dark Matter Origin of High Energy Positron Anomaly

Martin Pohl

*Institut für Physik und Astronomie, Universität Potsdam, 14476 Potsdam-Golm, Germany*

*DESY, 15738 Zeuthen, Germany*

pohlmadq@gmail.com

David Eichler

*Physics Department, Ben-Gurion University, Beer-Sheva 84105, Israel*

eichler@bgumail.bgu.ac.il

## ABSTRACT

Fermi measurements of the high-latitude  $\gamma$ -ray background strongly constrain a decaying-dark-matter origin for the 1–100 GeV Galactic positron anomaly measured with PAMELA. Inverse-Compton scattering of the microwave background by the emergent positrons produces a bump in the diffuse 100–200 MeV  $\gamma$ -ray background that would protrude from the observed background at these energies. The positrons are thus constrained to emerge from the decay process at a typical energy between  $\sim 100$  GeV and  $\sim 250$  GeV. By considering only  $\gamma$ -ray emission of the excess positrons and electrons, we derive a minimum diffuse  $\gamma$ -ray flux that, apart from the positron spectrum assumed, is independent of the actual decay modes. Any  $\gamma$ -rays produced directly by the dark-matter decay leads to an additional signal that make the observational limits more severe. A similar constraint on the energy of emergent positrons from annihilation in dark-matter substructures is argued to exist, according to recent estimates of enhancement in low-mass dark-matter substructures, and improved simulations of such substructure will further sharpen this constraint.

*Subject headings:* cosmic rays — dark matter — gamma rays: diffuse background

## 1. Introduction

The positron excess in Galactic cosmic ray positrons between 1 and 100 GeV, despite a history of conflicting results, appears to be confirmed by PAMELA (Adriani et al. 2009a). There are, of course, several possible astrophysical explanations. Nearby sources (e.g. supernova or pulsars) of positrons, for example, which suffer fewer losses than typical Galactic positrons because they are younger (e.g. Eichler & Maor 2005; Profumo 2008), contribute harder spectra. Nevertheless, dark matter annihilation (e.g. Tylka and Eichler 1987; Tylka 1989; Hooper et al. 2009) or decay (Eichler 1989; Arvanitaki et al. 2009) have long been suggested as a possible source.

Annihilation, however, encounters a number of difficulties, as it requires a substantial boosting either from clumping (e.g. Kuhlen & Malyshev 2009) or from a Sommerfeld enhancement (Arkani-Hamed et al. 2009), and would lead to intense photon emission from the Galactic-Center region (e.g. Eichler & Maor 2005; Zhang et al. 2009) or extragalactic background radiation from the superposition of haloes (Profumo & Jeltama 2009), that appears to exceed current observational limits.

Here we investigate dark-matter decay as the source of the excess positrons observed with PAMELA. Our purpose is not a comprehensive theory of the dark-matter decay, in particular not the viability of leptophilic decay, which is one of the challenges (Arkani-Hamed et al. 2009), given that standard hadronization scenarios are already excluded by the lack of an excess in the cosmic-ray antiproton data (Adriani et al. 2009b). The decay source function scales with the dark-matter density, not the density squared as does annihilation, and therefore the limits on decaying dark matter from observations of high-energy  $\gamma$  rays from, e.g., dwarf galaxies are weak (Essig et al. 2009), but diffuse emission may provide more stringent constraints (Ishiwata et al. 2009; Chen et al. 2009). We calculate the diffuse galactic  $\gamma$ -ray emission of the excess leptons, presuming they arise from dark-matter decay. The  $\gamma$ -ray intensity thus derived is more model-independent and also a lower limit to the true emission level, because we do not count  $\gamma$  rays that are directly produced in the dark-matter decay, possibly via other unstable particles.

## 2. Positron production by dark-matter decay

### 2.1. The differential number density of positrons

The propagation length of positrons and electrons at energies  $\gtrsim 50$  GeV is  $L_p \simeq 2\sqrt{\kappa \tau_{\text{loss}}} \lesssim 600$  pc (Pohl et al. 2003; Grasso et al. 2009), considerably less than the scale-

length of the dark-matter halo in the Galaxy, i.e. the source distribution of positrons and electrons from dark-matter decay. Here,  $\kappa$  is the energy-dependent diffusion coefficient and  $\tau_{\text{loss}}$  is the electron/positron energy-loss timescale. To first order, the spatial redistribution of those electrons by diffusive and convective transport can therefore be neglected. The differential number density of positrons has, in good approximation, the same spatial profile as the dark-matter density,  $\rho_{\text{DM}}$ , because in decay processes the positron source function obeys  $Q_{e^+} \propto \rho_{\text{DM}}$ . The differential number density of electrons/positrons in the steady state is then given by

$$N(E, \mathbf{x}) = \frac{1}{|\dot{E}(E)|} \int_E du Q_{e^+/e^-}(u) \quad (1)$$

Above 10 GeV electron energy, the electron energy-loss rate,  $\dot{E}(E)$ , is dominated by synchrotron and inverse Compton losses. The soft-photon density varies somewhat between the Galactic plane and the halo, reaching a maximum of  $1.5 \text{ eV/cm}^3$  about 300 pc above the mid-plane and falling to  $0.8 \text{ eV/cm}^3$  at 5 kpc above the midplane (Porter & Strong 2005). Here we use an average value  $U_{\text{ph}} = 1.1 \text{ eV/cm}^3$  to calculate the energy losses. The magnetic-field strength is not well known, and, using a canonical constant value for it,  $8 \mu\text{G}$ , we find for the energy-loss rate

$$\dot{E}(E) = -\frac{E}{\tau_{\text{loss}}} \simeq -(2.5 \cdot 10^{-14} \text{ GeV s}^{-1}) \zeta \left( \frac{E}{10 \text{ GeV}} \right)^2, \quad (2)$$

where we ignore the weak modifications arising from the Klein-Nishina corrections to the inverse-Compton scattering rate. The parameter  $\zeta$  permits a scaling of the energy-loss rate relative to that given by the model for the galactic radiation field and a magnetic-field strength  $B = 8 \mu\text{G}$ .

$$\zeta = \frac{U_{\text{ph}} + \frac{B^2}{8\pi}}{2.7 \text{ eV/cm}^3} \quad (3)$$

The microwave background implies a lower limit  $\zeta \geq 0.1$ , and a magnetic-field strength  $B = 5 \mu\text{G}$  would be described by  $\zeta = 0.64$ . Estimates of the Galactic magnetic field based on modeling the radio synchrotron emission give amplitudes from  $B = 6.1 \mu\text{G}$  (Strong et al. 2000) to  $B = 10 \mu\text{G}$  (Pohl & Esposito 1998), and the most likely value for  $\zeta$  is therefore in the range  $0.75 \leq \zeta \leq 1.3$ . The differential number density of electrons/positrons cannot have a spectrum harder than  $E^{-2}$ , which is the spectrum that comes from the hardest possible injection spectrum.

The PAMELA collaboration has measured a positron fraction that is rapidly increasing above 10 GeV. The highest-energy data point is

$$\frac{N_{e^+}}{N_{e^+} + N_{e^-}} (82 \text{ GeV}) = 0.137 \pm 0.045 \quad (4)$$

about 90% of which is in excess to the positrons expected from secondary production in cosmic-ray interactions. The total electron spectrum has not been determined with PAMELA yet, but we may use the excellent Fermi-LAT data that between 20 GeV and 1 TeV are well represented by a single power law (Abdo et al. 2009)

$$N_{e^+} + N_{e^-} = (73.5 \pm 2.6) \cdot 10^{-7} \left( \frac{E}{\text{GeV}} \right)^{-(3.045 \pm 0.008)} \text{ GeV}^{-1} \text{ m}^{-3} \quad (5)$$

Combining Eqs. 4 and 5 we find the positron density at 82 GeV as

$$N_{e^+}(82 \text{ GeV}) \simeq 1.5 \cdot 10^{-12} \text{ GeV}^{-1} \text{ m}^{-3} \quad (6)$$

The positron excess over ordinary secondary production is measured to be only about 0.03 at 17 GeV, thus indicating that the excess component has a spectrum not significantly softer than  $E^{-2}$ . Equation 1 indicates that this requires the injection of electron and positrons with a typical energy above 80 GeV. For simplicity we assume the injection of monoenergetic electrons,

$$Q_{e^+/e^-} = Q_0 \delta(E - E_{\text{max}}) \quad (7)$$

where  $E_{\text{max}} \lesssim 500 \text{ GeV}$  to avoid a spectral feature in the total electron spectrum, which would be in conflict with the power-law fit to the Fermi data. We shall see that the  $\gamma$ -ray limits calculated below provide much tighter constraints on  $E_{\text{max}}$ . Assuming an equal number of excess electrons and positrons, we therefore estimate the total differential density of electrons/positrons that may come from dark-matter decay as

$$N(E, \mathbf{x}) = (2.2 \cdot 10^{-8} \text{ GeV}^{-1} \text{ m}^{-3}) R(\mathbf{x}) \left( \frac{E}{\text{GeV}} \right)^{-2} \Theta(E_{\text{max}} - E) \quad (8)$$

In Figure 1 we demonstrate that the sum of this modeled dark-matter decay component and the expected contribution of secondary positron production provides a good fit to the PAMELA data. For comparison, the figure also displays the positron fraction for the case of a flat injection spectrum, which may result from the decay of an intermediate particle with high kinetic energy.

$$Q_{\text{alt.}} = \frac{Q_0}{E_0} \Theta(E_{\text{max}} - E) \quad (9)$$

$$\Rightarrow N_{\text{alt.}}(E, \mathbf{x}) \propto R(\mathbf{x}) \left( 1 - \frac{E}{E_{\text{max}}} \right) \left( \frac{E}{\text{GeV}} \right)^{-2} \Theta(E_{\text{max}} - E) \quad (10)$$

Here  $Q_0$  is chosen 20% larger than in the case of monoenergetic injection to improve the fit of the positron fraction. To be noted from the figure is that  $E_{\text{max}} \gtrsim 200 \text{ GeV}$  is needed for flat injection to well reproduce the positron fraction measured with PAMELA.

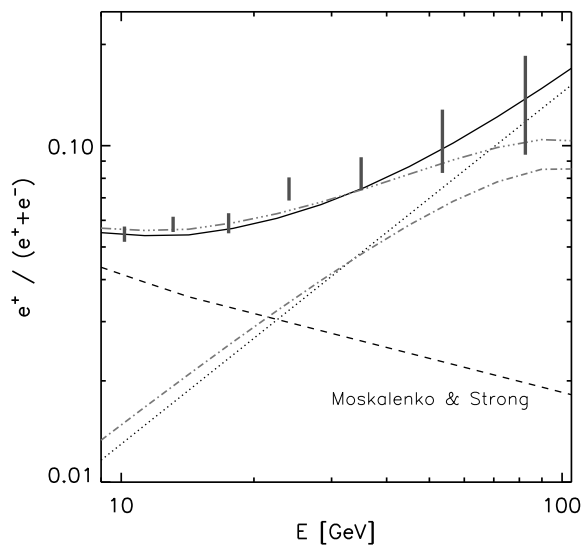


Fig. 1.— The measured positron fraction between 10 GeV and 82 GeV shown in comparison with a calculation for pure secondary production of positrons (Moskalenko & Strong 1998), the dark-matter contribution according to Eq. 8 (dotted line), and the total calculated positron fraction (solid line). For comparison, we also show the positron fraction for a flat injection spectrum up to 200 GeV (dot-dashed line) and the total positron fraction for that case (triple-dot-dashed line).

$R(\mathbf{x})$  denotes the spatial distribution normalized to the local density, which should reflect that of the dark-matter particles. Simulations suggest that the dark-matter halo in the Galaxy is not spherical, and the vertical scale height may be only 40% of that in the Galactic plane (Kuhlen et al. 2009). The tidal streams produced by the Sagittarius dwarf spheroidal may even indicate a triaxial density distribution (Law et al. 2009). Here we conservatively assume a dark-matter halo with vertical flattening and for simplicity a global  $r^{-2}$  density scaling instead of, e.g., a NFW halo (Navarro et al. 1996). In that approximation, the normalized density profile at the solar circle ( $r = R_0 = 8$  kpc) is

$$R(\mathbf{x}) = \frac{\rho(R_0, z)}{\rho(R_0, z=0)} \simeq \left(1 + 2.5 \frac{z^2}{R_0^2}\right)^{-1} \quad (11)$$

## 2.2. The dark-matter lifetime

Using Eqs. 1, 2, and 8 we can estimate the source function of pairs from dark matter, and hence the dark-matter decay timescale. Assuming for simplicity decay into monoenergetic pairs, we find from Equations 1 and 7

$$Q_0 = \zeta (5.5 \cdot 10^{-30} \text{ cm}^{-3} \text{ s}^{-1}) \quad (12)$$

The source power is

$$P = \int dE E Q_{e^+e^-} = Q_0 E_{\text{max}} = \zeta (1.1 \cdot 10^{-27} \text{ GeV cm}^{-3} \text{ s}^{-1}) \left(\frac{E_{\text{max}}}{200 \text{ GeV}}\right) \quad (13)$$

Comparing with the local dark-matter mass density,  $\rho_0 \simeq 0.3 \text{ GeV cm}^{-3}$ , and accounting for an arbitrary branching ratio of conversion into pairs,  $\eta$ , we find for the dark-matter decay time

$$\tau_{\text{decay}} = \frac{\rho_0 \eta}{P} \simeq \frac{\eta}{\zeta} (2.7 \cdot 10^{26} \text{ s}) \left(\frac{E_{\text{max}}}{200 \text{ GeV}}\right)^{-1} \quad (14)$$

Care must be exercised in comparing astrophysical limits on the decay time on account of its dependence on the energy of the injected pairs and on the assumed magnetic-field strength. For example, Chen et al. (2009) use  $B = 3 \mu\text{G}$ , implying  $\zeta = 0.5$ , and consequently their limits on  $\tau_{\text{decay}}$  are relatively high.

### 3. Inverse Compton scattering

#### 3.1. Galactic emission

The electrons and positrons in the halo will inverse-Compton scatter soft photons into the  $\gamma$ -ray band where they can be observed with, e.g., the Fermi-LAT detector. The target photon field includes the microwave background, galactic infrared emission, and galactic optical emission, only the first of which is isotropic. The latter two will be backscattered toward the Galaxy, thus somewhat increasing the scattering rate compared with the isotropic case. The radiation field has been recently modeled out to  $z = 5$  kpc (Porter & Strong 2005). Surprisingly, the energy density of optical light is higher in the halo than in the midplane on account of the thin-disk distribution of absorbers.

The differential cross section for the up-scattering of isotropic photons of energy  $\epsilon$  to energy  $E_\gamma$  is given by (Blumenthal & Gould 1970)

$$\sigma(E_\gamma, \epsilon, E) = \frac{3 \sigma_T (m_e c^2)^2}{4 \epsilon E^2} \left[ 2 q \ln q + 1 + q - 2 q^2 + \frac{(1 - q) q^2 \Gamma_e^2}{2 (1 + q \Gamma_e)} \right] \quad (15)$$

where

$$q = \frac{E_\gamma}{\Gamma_e (E - E_\gamma)} \quad \text{and} \quad \Gamma_e = \frac{4 \epsilon E}{m_e^2 c^4} \quad (16)$$

The  $\gamma$ -ray intensity observed from the Galactic pole is then computed using the differential density of electrons/positrons (Eq. 8) and the differential density of soft photons,  $n(\epsilon)$  (Porter & Strong 2005).

$$I_\gamma = \frac{c}{4\pi} \int_0^z dz \int dE N(E, \mathbf{x}) \int d\epsilon n(\epsilon) \sigma(E_\gamma, \epsilon, E) \quad (17)$$

The resulting intensity is shown in Figure 2. To be noted from the figure is that even at 30 GeV, where the emission arises from upscattering optical photons, the expected intensity is below 20% of the preliminary estimate of the extragalactic isotropic background observed with Fermi (Ackermann 2009), in line with the findings of Ishiwata et al. (2009). Diffuse galactic emission from cosmic-ray interaction has an intensity similar to that of the extragalactic isotropic background, and hence dark-matter decay is poorly constrained by  $\gamma$ -ray emission in the Galaxy.

Whereas no significant intensity above 1 GeV is expected to come from beyond a distance of 5 kpc, the limit to which we have integrated the galactic emission, this is not true for the upscattering of microwave-background photons into the 100-MeV band. In fact, in the outer halo inverse-Compton scattering of the microwave background accounts for a larger share of the electron energy losses than near the Galactic plane, because the infrared and

optical photon fields quickly lose intensity beyond 5 kpc above the plane of the Galaxy. Also, the magnetic-field strength is expected to fall off, although we do not know at what point it drops to  $3 \mu\text{G}$ , below which the synchrotron energy losses are subdominant. We will estimate the intensity in the 100-MeV band from galactic dark-matter decay in the outer halo in the next section, together with the extragalactic component.

### 3.2. Extragalactic background from intergalactic dark matter

The majority of dark matter is located sufficiently far away from galaxies ( $\gtrsim 20$  kpc) that positrons and electrons from its decay would primarily interact with the microwave background. Since all electrons suffer the same fate and the electron source rate scales linearly with the dark-matter density, we can ignore any density structure and use spatially averaged quantities, i.e. a conservative fraction 90% of  $\Omega_m = 0.239$  times the critical density,  $9.9 \cdot 10^{-30} \text{ g cm}^{-3}$ . For the source function and the energy-loss rate we find

$$Q_{e^+/e^-} \simeq (1+z)^3 \zeta (2.2 \cdot 10^{-35} \text{ cm}^{-3} \text{ s}^{-1}) \delta(E - E_{\text{max}}) \quad (18)$$

and

$$\dot{E} = (1+z)^4 (-2.5 \cdot 10^{-17} \text{ GeV s}^{-1}) \left( \frac{E}{\text{GeV}} \right)^2 \quad (19)$$

where  $z$  denotes the redshift. The average differential number density is therefore

$$N(E, z) = \frac{\zeta}{1+z} (8.8 \cdot 10^{-19} \text{ GeV}^{-1} \text{ cm}^{-3}) \left( \frac{E}{\text{GeV}} \right)^{-2} \Theta(E_{\text{max}} - E) \quad (20)$$

The intensity of inverse-Compton emission is calculated as

$$I_\gamma = \frac{c}{4\pi (1+z)^2} \int_0^1 dz f(z) \int dE N(E, z) \int d\epsilon n(\epsilon) \sigma [E_\gamma (1+z), \epsilon, E] \quad (21)$$

where

$$f(z) = \frac{c}{H_0 (1+z)} \left[ (1+z)^2 (1 + \Omega_m z) - z (2+z) \Omega_\Lambda \right]^{-\frac{1}{2}} \quad (22)$$

is the Jacobian used to turn the line-of-sight integral into a redshift integral. We integrate to redshift  $z = 5$ , beyond which the emissivity is negligibly small. The soft-photon distribution is the cosmological microwave background

$$n(\epsilon) = \frac{8\pi \epsilon^2}{h^3 c^3} \frac{1}{\exp\left(\frac{\epsilon}{\epsilon_0 (1+z)}\right) - 1} \quad (23)$$



with  $\epsilon_0 = 2.4 \cdot 10^{-4}$  eV, added to which is a small contribution in the infrared band (Franceschini et al. 1998). The resulting expected  $\gamma$ -ray intensity is plotted in Figure 2 for  $\zeta = 1$ , together with that produced in the outer parts of the Milky-Way halo at height  $z \geq 10$  kpc where IC scattering off the CMB is also dominant and the expected differential density of electrons and positrons from dark-matter decay is

$$N(E, \mathbf{x}) = (2.4 \cdot 10^{-7} \text{ GeV}^{-1} \text{ m}^{-3}) R(\mathbf{x}) \left( \frac{E}{\text{GeV}} \right)^{-2} \Theta(E_{\text{max}} - E) , \quad (24)$$

larger than the galactic-plane solution (Eq. 8) by the ratio of the energy-loss lifetime in the outer halo to that in the galactic plane. If the excess electrons and positrons could freely stream in the outer halo, we would be overestimating their  $\gamma$ -ray emission which contributes at most 1/3 of the total dark-matter signal. However, a number of well-known plasma instabilities would sharply impede such free streaming. As a 100-GeV electron has a propagation length of only  $\sim 15$  kpc even if the diffusion coefficient is a 100 times that in the galactic plane, the effect of particle propagation is neglected in deriving Eq. 24.

At 200 MeV  $\gamma$ -ray energy, the predicted intensity is close to that observed with Fermi (Ackermann 2009). The uncertainty in the measured intensity is typically 15% and predominantly systematic in origin. Because the electron/positron density is linear in  $\zeta$ , the predicted  $\gamma$ -ray intensity would exceed the observational limits if the total magnetic-field in the solar vicinity were stronger than  $10 \mu\text{G}$ . It would also exceed the observational limits if the characteristic energy of the injected pairs were higher than  $\sim 250$  GeV. For comparison, Figure 2 also shows the expected intensity for  $E_{\text{max}} = 300$  GeV to be twice that observed at 200 MeV  $\gamma$ -ray energy.

The same scaling with energy  $E_{\text{max}}$  results for flat injection (cf. Eqs. 9 and 10). The  $\gamma$ -ray peak will appear at slightly lower energy and with somewhat reduced flux compared with monoenergetic injection at the same  $E_{\text{max}}$ , because the mean particle energy is  $E_{\text{max}}/2$ . This is demonstrated as well in Figure 2 where we show the expected  $\gamma$ -ray bump resulting from flat injection up to 300 GeV, i.e. with characteristic energy  $\sim 150$  GeV.

## 4. Conclusions

We have investigated  $\gamma$ -ray constraints on the notion that dark-matter decay is responsible for the recently measured excess of cosmic-ray positrons in the 1–100 GeV band. While the predicted GeV-band intensity from the inverse-Compton scattering of infrared and optical photons is below a preliminary estimate of the extragalactic  $\gamma$ -ray background based on Fermi data (Ackermann 2009), the *extragalactic* background from the decay of intergalactic dark matter would produce a bump at 100–300 MeV that is close to the observed

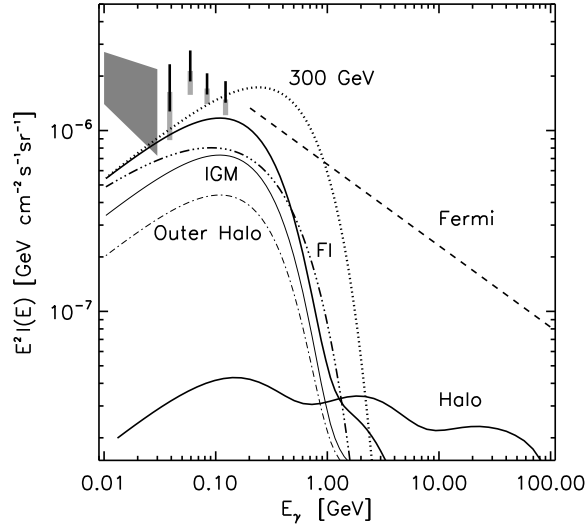


Fig. 2.— Comparison of the predicted  $\gamma$ -ray intensity observed from the galactic poles with the preliminary estimate of the extragalactic isotropic background observed with Fermi, indicated by the dashed line (Ackermann 2009), and older data from COMPTEL (Kappadath 1999) and EGRET (Sreekumar et al. 1998; Strong et al. 2004). The thick line labeled Halo shows galactic emission according to equation 17, and the other lines are for  $\gamma$ -ray emission from intergalactic dark matter, all for  $\zeta = 1$  and except where noted for  $E_{\max} = 200$  GeV. In detail, the thin solid line is extragalactic emission as given in equation 21, the dot-dashed line is emission from the outer Milky-Way halo beyond  $z = 10$  kpc, the thick solid line the sum of the two, and the dotted line is the same for  $E_{\max} = 300$  GeV. The triple-dot-dashed line labeled FI is for flat injection up to 300 GeV (cf. Eqs. 9 and 10).

extragalactic background at these energies, even one estimated from the older EGRET data (Sreekumar et al. 1998). Dark-matter decay therefore does not seem to be a viable explanation of the positron excess, unless the characteristic energy of the pairs produced in dark-matter decay is only in a narrow window between the lower limit  $\sim 100$  GeV imposed by high-energy limit of the Pamela measurement and the high energy limit of  $\sim 250$  GeV imposed by the extragalactic 100 to 200 MeV  $\gamma$ -ray background.

Our stated limits are conservative in several ways: a) Any  $\gamma$  rays directly produced in the decay of the dark-matter particles will lead to an additional signal that will make the observational limits more severe. b) We have neglected the contribution of astrophysical sources that are needed to explain the *shape* of the observed  $\gamma$  ray spectrum, which is far broader than the dark-matter contribution. Any dark matter contribution would probably be noticeable at the 30 percent level. c) Any real decay process may involve multi-generational pairs, such as decay into electron positron pairs via taus and muons, even if quarks are avoided by some leptophilic process. This makes it harder to fit the pairs into the allowed energy window.

We stress that the predicted 100-200 MeV  $\gamma$ -ray intensity from dark-matter decay is nearly model-independent, because it depends only on the total dark-matter density in regions outside those of strong galactic magnetic fields and starlight, i.e. in regions where inverse-Compton scattering of microwave background photons is a calorimeter for intergalactic electrons and positrons on account of its dominance among the energy-loss processes. The only assumptions we have made are time-independence of the dark-matter lifetime, which follows from conventional elementary particle physics, and the best estimates for the average magnetic field of the Galaxy in the solar neighborhood.

Moreover, because the anomalous positrons reported by PAMELA are too energetic to retain their energy for a Hubble time, the only way to prevent the energy from going into  $\gamma$  rays is to preempt the inverse Compton losses with even faster synchrotron losses. It would seem then that magnetic fields of strength  $\gtrsim 3 \mu\text{G}$  are the only way to preempt IC losses.

The argument would then apply to positrons from clump-enhanced dark matter annihilation as well as decay, if such enhancement occurred a) mostly in the outer part of galaxies where the magnetic field and starlight are weak, b) in extragalactic dark matter clumps or dwarf galaxies, where the magnetic field is weaker than in our own galaxy or c) elliptical galaxies, where the magnetic field strengths are likely to be less than in our own Galaxy. Quantifying this constraint for annihilating dark matter requires a reliable computation of the distribution of annihilation, which is limited by numerical resolution at small mass scales. Diemand et al. (2007) argue that the positron emissivity per unit mass ( $q$ ) in the outer halo,  $q_{oh}$ , exceeds that in the local galactic neighborhood,  $q_{ln}$ , because substructure

survives tidal destruction far better there. This would raise the  $\gamma$  ray contribution in the outer halo by a factor of  $q_{oh}/q_{ln}$  relative to the limits we derive for decaying dark matter, where  $q_{oh}/q_{ln} = 1$  everywhere. Extragalactic substructure may give an even higher  $q$ , because there is less tidal destruction, though there is the competing effect that in regions of lower density fluctuation, substructure is less likely to form at high redshift. Sommerfeld enhancement of the annihilation cross section at low center-of-mass energy would further raise the contribution of low mass substructures, in which the center-of-mass kinetic energy of the annihilating pairs would be lower than in the diffuse dark matter in the solar neighborhood (Kuhlen, Madau, and Silk 2009; Kistler & Siegal-Gaskins 2009). Thus, if we could make reliable simulations of dark-matter substructure down to the smallest mass scales for all cosmic locations, the results would probably already rule out explaining the PAMELA positron excess by annihilating dark matter.

The arguments here do not, of course, immediately rule out detection of decay or annihilating dark matter by other more sensitive means, e.g.  $\gamma$  rays from localized DM concentrations. They merely argue against most scenarios for explaining the PAMELA positron anomaly in this manner. However, they call attention to the fact that any scenario for making  $\gamma$  rays that includes accompanying  $e^+ e^-$  pairs, e.g.  $\gamma$  rays by pion decay or final state radiation, may be constrained by the inverse Compton  $\gamma$  rays that would accompany the direct  $\gamma$  rays emitted in regions of weak magnetic field. Conversely, annihilation or decay that produces more pairs than direct  $\gamma$  rays may be more readily detected via inverse Compton radiation of the pairs.

We thank M. Kuhlen and P. Madau for helpful discussions. We acknowledge support from the U.S.-Israel Binational Science Foundation, the Israel Academy of Science, and the Robert and Joan Arnow Chair of Theoretical Astrophysics. This research was supported in part by the National Science Foundation under Grant No. PHY05-51164.

## REFERENCES

- Abdo, A.A. et al. (The Fermi collaboration) 2009, PRL 102, 181101
- Ackermann, M., for the Fermi collaboration, 2009, Talk at International Cosmic Ray Conference, Lodz, Poland
- Adriani, O., Barbarino, G.C., Bazilevskaya, G.A., et al. 2009a, Nature 458, 607
- Adriani, O., Barbarino, G.C., Bazilevskaya, G.A., et al. 2009b, PRL 102, 051101

- Arkani-Hamed, N., Finkbeiner, D.P., Slatyer, T.R., Weiner, N. 2009, PRD 79, 015014
- Arvanitaki, A. Dimopoulos, S., Dubovsky, S., Graham, P.; Harnik, R., Rajendran, S. 2009, Phys. Rev. D80.055011
- Blumenthal, G.R. Gould, R.J. 1970, Rev. Mod. Phys. 42-2, 237
- Chen, C.R., Mandal, S.K., Takahashi, F. 2009, (arXiv:0910.2639v2)
- Diemand, J., Kuhlen, M., and Madau, P. 2007, ApJ 657, 252
- Eichler, D. 1989, PRL 63, 2440
- Eichler, D., and Maor, I. 2005, (arXiv:astro-ph/0501096)
- Essig, R., Sehgal, N., Strigari, L.E. 2009, PRD 80, 223506
- Franceschini, A., Rodighiero, G., Vaccari, M. 2008, A&A 487, 837
- Grasso, D., Profumo, S., Strong, A.W., et al. 2009, Astrop. Phys. 32, 140
- Hooper, D., Stebbins, A., Zurek, K.N. 2009, PRD 79, 103513
- Ishiwata, K. Matsumoto, S., Moroi, T. 2009, Phys. Lett. B 679-1, 1
- Kappadath, S.C. 1999, Ph.D. Thesis, University of New Hampshire
- Kistler, M.D., Siegal-Gaskins, J.M. 2009, arXiv:0909.0519
- Kuhlen, M., & Malyshev, D. 2009, PRD 79, 123517
- Kuhlen, M., Diemand, J., Madau, P. 2007, ApJ 671, 1135
- Kuhlen, M., Madau, P., & Silk, J. 2009, Science, 325, 970).
- Law, D.R., Majewski, S.R., Johnston, K.V. 2009, ApJ 703, L67
- Moskalenko, I.V., Strong, A.W. 1998, ApJ 493, 694
- Navarro, J.F., Frenk, C.S., White, S.D.M. 1996, ApJ 462, 563
- Pohl, M., Perrot, C., Grenier, I., Digel, S. 2003, A& A 409, 581
- Pohl, M., Esposito, J.A. 1998, ApJ 507, 327
- Porter, T.A. & Strong, A.W. 2005, Proc. of the 29th ICRC, Pune, (arXiv:astro-ph/0507119)

Profumo, S., Jeltema, T.E. 2009, JCAP 07, 020

Profumo, S. 2008, arXiv:0812.4457v2

Sreekumar, P., Bertsch, D.L., Dingus, B.L., et al. 1998, ApJ 494, 523

Strong, A.W., Moskalenko, I.V., Reimer, O. 2004, ApJ 613, 956

Strong, A.W., Moskalenko, I.V., Reimer, O. 2000, ApJ 537, 763

Tylka, A.J and Eichler, D. (2007) U. Md. Technical Report,

Tylka, A.J. 1989, PRL 63, 40

Zhang, J. et al. 2009, PRD 80, 023007